
Observational Constraints on the Modified Gravity Model (MOG) Proposed by Moffat: Using the Magellanic System

Hosein Haghi and Sohrab Rahvar

the date of receipt and acceptance should be inserted later

Abstract A simple model for the dynamics of the Magellanic Stream (MS), in the framework of modified gravity models is investigated. We assume that the galaxy is made up of baryonic matter out of context of dark matter scenario. The model we used here is named Modified Gravity (MOG) proposed by Moffat (2005). In order to examine the compatibility of the overall properties of the MS under the MOG theory, the observational radial velocity profile of the MS is compared with the numerical results using the χ^2 fit method. In order to obtain the best model parameters, a maximum likelihood analysis is performed. We also compare the results of this model with the Cold Dark Matter (CDM) halo model and the other alternative gravity model that proposed by Bekenstein (2004), so called TeVeS. We show that by selecting the appropriate values for the free parameters, the MOG theory seems to be plausible to explain the dynamics of the MS as well as the CDM and the TeVeS models.

PACS numbers: 05.10.-a, 05.10.Gg, 05.40.-a, 98.80.Es, 98.70.Vc

1 Introduction

The asymptotic flattening of rotation curves of disk galaxies has been explained by invoking still undetected forms of non-baryonic dark matter [1,2]. Dark matter in the form of halo, has been successfully proposed to explain the dynamics of clusters of galaxies, gravitational lensing and the standard model of cosmology within the framework of general relativity. Although the currently favored Cold Dark Matter (CDM) model has proven to be remarkably successful on large scales [3], dark matter has not yet been detected after several experimental efforts. Furthermore, high resolution N-body simulations are still in contradiction with the observations on subgalactic scales: the simulations predict more satellites than what is seen [4,5], and the implied spatial distribution of sub-halos is in contradiction with observation[6]. However, newly dis-

Hosein Haghi
Institute for Advanced Studies in Basic Sciences (IASBS), P. O. Box 45195-1159, Zanjan, Iran
Sohrab Rahvar
Department of Physics, Sharif University of Technology, P.O.Box 11365-9161, Tehran, Iran

covered galaxies in SDSS and new simulations considering the environmental effect on the sub-halo abundance have significantly removed this discrepancy [7, 8, 9].

In order to explain the missing matter of the Universe, other alternative theories of gravity have been proposed. In these models, modification of the laws of gravitation can explain the observed asymptotically flat rotation curve of galaxies without invoking dark matter. One of the most famous alternative theories is the Modified Newtonian Dynamics (MOND) which has been introduced by Milgrom [10]. According to this phenomenological theory, the flat rotation curves of spiral galaxies are explained by modification of Newton's second law for acceleration below the characteristic scale $a_0 = 1.2 \times 10^{-10} \text{ m s}^{-2}$ [11, 12, 13]. Recently, TeVeS¹, a Lorentz-covariant version of MOND, has been presented [14]. It cannot explain the internal dynamics and merging of galaxy clusters such as the "Bullet Cluster" without invoking special forms of dark matter [15, 16].

Modified Gravity (MOG) is another alternative theory which has been proposed by Moffat (2005)[17, 18, 19]. It is a fully relativistic theory of gravitation which is derived from a relativistic action principle involving scalar, tensor and vector fields. This theory explained successfully a large number of galactic rotation curves, the mass and thermal profiles of clusters of galaxies, the recent data of merging clusters, and the CMB acoustical power spectrum data [27, 28, 29, 30].

The dynamics of the satellite galaxies and globular clusters around the Milky Way could be another approach to examine alternative gravity models [31, 33]. In order to discriminate, at least in principle, between CDM, MOG and MOND theories, recently the orbital history of Magellanic Clouds (MCs) and 3D Sun's motion in the Milky Way have been studied by Iorio [34, 35]. The consistency of the dynamics of Magellanic Stream (MS, a narrow band of neutral hydrogen clouds started from the MCs and oriented towards the south galactic pole)[37, 38] in MOND theory has been investigated in our previous work [31]. Here we generalize that work to test MOG and compare it with the results obtained with the TeVeS and CDM model.

In this paper, we use a tidal model for the formation and evolution of the MS. We study the dynamics of MS for different galactic models and compare the radial velocity with the observational data. Modified gravitational effect of galactic disk as the luminous part of the MW is used to study the dynamics of the MS in the context of the MOG and the TeVeS. The results are compared with those obtained by including dark matter halo under the conventional Newtonian gravity. In this work we use six different sets of initial conditions that have been reported in literature (Table 1). For each set of initial conditions we run a large number of simulations with different galactic potentials and compare the outcomes to the observation. The paper is organized as follows. In section 2 we give a brief review on the dark halo and disk model of the MW. In section 3 we introduce the TeVeS and the MOG models. The modeling and dynamics of the MS are reviewed in section 4. Results and discussion are given in section 5. The paper is concluded in section 6.

¹ Tensor-Vector-Scalar

2 Galactic model

We use the Kuzmin potential for galactic disk. The Newtonian potential for infinitesimally thin Kuzmin disc is given by

$$\Phi_N(R, z) = \frac{-GM}{\sqrt{R^2 + (a + |z|)^2}}, \quad (1)$$

where $a = 4.5$ kpc is the scale length and $M = 1.2 \times 10^{11} M_\odot$ is the mass of the disk [54].

In order to compare the results with the prediction of CDM theory, we add an axisymmetric logarithmic halo whose the gravitational potential is [49]

$$\Phi_G^{(L)} = -\frac{1}{2}V_0^2 \log(R_c^2 + R^2 + z^2q^{-2}), \quad (2)$$

where, R_c is the core radius, V_0 is the asymptotic velocity and q is the flattening parameter: $q = 1$ represents a spherical halo and $q \neq 1$ gives an elliptical halo. Different total masses of the Milky Way in the form of halo give rise to different values of V_0 . Therefore, there are different values of V_0 in the literature: $V_0 = 161 \text{ kms}^{-1}$ that is used by Jonston et al (1999) and Law et al (2005) [52, 53], $V_0 = 175 \text{ kms}^{-1}$ that Read and Moore (2005)[54] used to reproduce the tidal feature of Sagittarius, or $V_0 = 210 \text{ kms}^{-1}$ that Kochanek (1996)[55] obtained from an analysis of the orbital motion of Galactic satellites. In agreement with Helmi (2004)[56] and Ruzicka et al. (2007)[66], we set $V_0 = 185 \text{ kms}^{-1}$ and $R_c = 12$ kpc which well reproduced the kinematics of the Magellanic Stream.

We choose the logarithmic potential for several reasons. First, the relatively small number of input parameters of Eq.2 makes the numerical calculations faster. Secondly, the logarithmic potential was employed in a recent study of dwarf galaxy streams to investigate the MW dark matter halo [56], and thus the application of the same formula allows for comparison of our results. In addition, it allows for the investigation of non spherical model of the Galactic halo. Finally, the flattened logarithmic halo model is very nearly identical to the potential of Kuzmin disk in the deep-MOND regime (see section 3).

3 MOG and TeVeS

MOG consists of three theories of gravity called the nonsymmetric gravity theory (NGT), the metric-skew-tensor gravity (MSTG) theory, and the scalar-tensor-vector gravity (STVG). MOG has been proposed by Moffat to explain the rotation curves of galaxies, clusters of galaxies and cosmology without dark matter [17, 18, 19, 20, 21, 22, 23, 24, 25]. It was shown that a parameter-free version of STVG can be obtained from an action principle [26]. Good fits to astrophysical and cosmological data have been obtained with this more recent version of STVG. An important feature of the NGT, MSTG, and STVG theories is that the modified acceleration law for weak gravitational fields has a Yukawa-shape force added to the Newtonian acceleration law. However, MOG has encountered problems in the solar system [36]. In the weak field approximation limit, STVG, NGT and MSTG produce similar results. From the field equations derived from the MOG action, one can obtain the modified Newtonian acceleration law for weak gravitational fields as [19, 30]

$$g_M = \frac{G(r)M(r)}{r^2} \quad (3)$$

$$G(r) = G_N \times \left\{ 1 + \alpha(r) \left[1 - e^{-r/r_0} \left(1 + \frac{r}{r_0} \right) \right] \right\}, \quad (4)$$

where $G(r)$ is the effective gravitational coupling constant, G_N is the Newtonian gravitational constant, M is the baryonic mass, and $\alpha(r) = \sqrt{M_0 M^{-1}}$. Because of the large galactocentric distance of LMC, we use the point mass approximation for the total stellar mass (disk and bulge). The masses of the disk and the bulge are $M_{disk} = 10^{11} M_\odot$, $M_{bulge} = 3.4 \times 10^{10} M_\odot$, yielding a total baryonic mass of $M = 1.34 \times 10^{11} M_\odot$ [53]. Moreover, $M_0(r)$ and $r_0(r)$ are two scaling parameters that vary with distance and determine the coupling strength of the vector field to baryonic matter and the range of the force, respectively. These parameters are determined by the equations of motion for effective scalar fields derived from an action principle [19]. In order to calculate the MOG dynamics, we have to phenomenologically obtain M_0 and r_0 : this determines $G(r)$. It is postulated that M_0 and r_0 give the magnitude of the constant acceleration as

$$g_0 = \frac{GM_0}{r_0^2}. \quad (5)$$

We assume that, for galaxies and galaxy clusters this acceleration is determined by $g_0 = cH_0$, where $H_0 = 100h \text{ km s}^{-1} \text{ Mpc}^{-1}$ is the current measured Hubble constant and $h = (0.71 \pm 0.07)$. This gives $g_0 = 6.90 \times 10^{-10} \text{ m s}^{-2}$.

Analyzing the galaxy rotation curves, a satisfactory fit to LSB and HSB galaxy data is obtained with the parameters $M_0 = 9.6 \times 10^{11} M_\odot$ and $r_0 = 13.9 \text{ kpc}$, whereas in the dwarf galaxies smaller than 12 kpc, the best fit value of parameters obtained as $M_0 = 2.4 \times 10^{11} M_\odot$ and $r_0 = 9.7 \text{ kpc}$, and for the satellite galaxies, the parameters are $M_0 = 4.6 \times 10^{13} M_\odot$ and $r_0 = 111.3 \text{ kpc}$ [28]. An empirical fitting of M_0 versus r_0 for the wide range of spherically symmetric systems, from the solar system scale to clusters of galaxies has been obtained and depicted in Fig. 2 of [30]. The modifications to gravity in Eq. (3) would be canceled by decreasing M_0 and increasing r_0 (i.g. $M_0 \rightarrow 0$ and $r_0 \rightarrow \infty$). These parameters are scale dependent; thus, they are not to be taken as universal constants. MOG is not arisen from a classical modification, but from the equations of motion of a relativistic modification to general relativity.

According to TeVeS model, the physical metric near a quasi-static galaxy is given by the same metric as in general relativity with just a little change: the Newtonian potential for known matter, ϕ_N replaced by the total Φ which comes from two parts,

$$\Phi = \Phi_N + \phi_s, \quad (6)$$

where, ϕ_s is a potential due to a scalar field. The added scalar field plays the role of the dark matter gravitational potential and the corresponding modified acceleration is $g = g_N + g_s$. The scalar field potential for the Kuzmin disk is as following [51]

$$\phi_s \simeq \frac{(MGa_0)^{1/2}}{2} \ln(R^2 + (|z| + a)^2). \quad (7)$$

From Eqs. (1), (6) and (7), we calculate the accelerations of a test object orbiting the galaxy.

Because the Poisson's equation is non-linear in MOND, the strong equivalence principle is violated [11], and consequently the internal properties and the morphology

of a stellar system are affected both by the internal and external fields. This effect is specific for MOND; it significantly affects non-isolated systems and, in principle, it should be taken into account.

In the presence of an external field, the total acceleration, which is the sum of the internal a_i and external a_e accelerations, satisfies the modified Poisson equation [11]

$$\nabla \cdot [\mu(\frac{|\mathbf{a}_i + \mathbf{a}_e|}{a_0}) (\mathbf{a}_i + \mathbf{a}_e)] \simeq 4\pi G\rho, \quad (8)$$

where \mathbf{a}_e approximately is constant, $\mathbf{a}_i = \nabla\phi$ is the non-external part of the potential, and ρ is the density of the star cluster. For spherical system one can approximately write equation 8 as $\mathbf{a}_i \mu(|\mathbf{a}_i + \mathbf{a}_e|/a_0) = \mathbf{a}_N$. The EFE is indeed a phenomenological requirement of MOND and it was postulated by Milgrom (1983) to explain the dynamical properties of nearby open clusters in MW. Equation 8 is only an approximate way to take into account the external field effect, in order to avoid from solving the modified Poisson equation with an external source term ρ_{ext} on the right-hand side. The EFE allows high velocity stars to escape from the potential of the Milky Way [58, 59], and implies that rotation curves of spiral galaxies should fall where the internal acceleration becomes equal to the external acceleration [60,61].

In the three body problem of LMC-SMC-MW interaction, the external field of MW plays an important role in the internal interaction of LMC and SMC as MONDian EFE (for more details see the paper by Iorio [34]). Since the used model for magellanic system in this paper is the single cloud model (i.e. we neglect the presence of SMC), there is no mutual interaction between Clouds, and therefore we do not consider the EFE in the orbital motion of LMC. In the next section using the RK4 technique we solve numerically the equations of motion.

4 Modeling and Dynamics of Magellanic System

The Magellanic Stream is due to past LMC-SMC-MW interaction; it extends along a curved path as a narrow band of neutral hydrogen clouds, originating from the MCs and oriented towards the south galactic pole [37, 38]. The radial velocity and the column density of this structure has been measured by many groups [39, 40]. The observed HI radial velocity profile is measured along the Magellanic Stream in the Galactic Standard of Rest (GSR) frame (see caption of Table 1). Large-area 21-cm² radio surveys have produced most of the information now available about the detailed structure of the MS. Since its discovery as a long stream of HI gas trailing the MCs, a number of models have attempted to explain the dynamics and origin of the MS. Observations show that the radial velocity of the MS with respect to the Galactic center changes from 0 kms⁻¹ at the beginning to -200 kms⁻¹ at the end of the tail.

There are two main explanation for the origin of the MS: the tidal-stripping [42, 43, 44, 45, 62, 63] and the ram-pressure model [46, 47, 48, 64, 65, 66]. According to the tidal hypothesis, the interaction of the MCs with the MW turns out the materials to form the tidal tails emanating from opposite side of the Clouds. In the tidal scenario, although the observed radial velocity profile of the stream has been modeled remarkably well,

² The electron and proton in the hydrogen atom can have their spins parallel or antiparallel. A transition between these two states is called a spin-flip transition and leads to the emission of a photon whose wavelength is 21 cm. This is in the radio part of the electromagnetic spectrum.

IC	3D $v(x, y, z)(km/s)$	$r(x, y, z)(kpc)$
GN96	(-5,-226,194)	(-1.0,-40.8,-26.8)
HR94	(-10.06,-287.09,229.73)	(-0.8,-40.8,-27.9)
K2	(-91,-250,220)	(-0.8,-41.5,-26.9)
K1 Mean	(-86 ± 12, -268 ± 11, 252 ± 16)	(-0.8,-41.5,-26.9)
M05	(-4.3,-182.45,169.8)	(0,-43.9,-25.1)
vdM02	(-56 ± 36, -219 ± 23, 186 ± 35)	(-0.8,-41.5,-26.9)

Table 1 The LMC initial conditions (IC) in Galactocentric coordinates which is a right-handed Cartesian system with the origin at the galactic center, the galactic plane at $Z = 0$ and the sun at the position $R_{\odot} = (-7.9, 0, 0)$. References: Gardiner & Noguchi (1996, GN96), Heller & Rohlfs (1994, HR94), Kallivayalil et al. (2006a,b, K1 and K2), Mastropietro et al. (2005, M05), and van der Marel et al (2002, vdM02).

the smooth HI column density distribution does not agree with the observations and the expected stars in the stream have not been observed yet.

The other hypothesis invokes the idea of ram pressure stripping of gas from the MCs by an extended halo of diffused gas around the Galaxy. The drag force on the gas between the MCs causes weakly bound material to escape and form a trailing gaseous stream. This material after escaping from the MCs falls towards the Galaxy. On the other hand, also the ram pressure models have their own problems. The clumpy structure of the Stream can hardly be reproduced by the process of continuous ram pressure stripping and can not reproduce the observed slope of the radial velocity profile along the MS, especially the high negative velocity tip of the Stream. Naturally, if the gas in the galactic halo has a clumpy distribution, which seems likely, this would lead to a clumpy MS in the ram pressure scenario.

In this section we calculate the dynamics of MCs in modified gravity theories, using their its present positions and velocities as the initial conditions for the equations of motion. The overall external force on the MCs is the sum of the gravitational pull by the Galactic halo and disk, hydrodynamical drag force from the extended gaseous halo and dynamical friction force from the Galactic halo. In MOG and TeVeS models, since we have ignored the Galactic halo, there is no dynamical friction and the main factor in the gas stripping is the tidal force exerted by the Galactic disk. It should be noted that, in the absence of extended dark halo, dynamical friction produces if an object moves through the visible mass distribution of the host galaxy. There is no dynamical friction for an object that moves outside the mass distribution. In the case of MCs, since the Clouds move very far from the center of the MW (i.e. outside the visible mass distribution), there is no dynamical friction in the equations of motion. The general equation of motion of the MCs is

$$\frac{d^2 \mathbf{r}_c}{dt^2} = \frac{\partial}{\partial r_c} [\phi_G(r_c)] + \frac{\mathbf{f}_c + \mathbf{F}_{drag}}{m_c}, \quad (9)$$

where, \mathbf{r}_c is the distance of the MCs from the Galactic center, m_c is the mass of the Cloud, ϕ_G is the gravitational potential of the Galaxy, \mathbf{f}_c is the dynamical friction force, and \mathbf{F}_{drag} is the hydrodynamical drag force. We adopt the standard form of dynamical friction as follows [57]

$$\mathbf{f}_c = 0.428 \ln \Lambda \frac{G m_c^2}{r^2} \frac{\mathbf{v}_c}{v_c}, \quad (10)$$

where $\ln A \sim 3$ is the coulomb logarithm and v_c is the relative speed with respect to the gaseous halo. Here we model the MCs with a dense sphere moving through the gaseous halo; thus the drag force on this sphere is given by

$$F_{drag} = \frac{1}{2} C_d \rho_g v_c^2 \pi D^2, \quad (11)$$

where C_d is the coefficient of drag force, ρ_g is the density of halo and D is the size of the MCs. The drag force plays no significant role in the orbital motion of LMC [32]. Therefore, we will neglect the drag force for the rest of the paper.

One of the problems with modeling the MCs–MW interaction is an extended high dimensional parameter space. In order to reduce the parameter space, one can neglect the influence of the SMC in the LMC-SMC-MW interaction (single cloud model). Lin & Lynden-Bell [67] showed that such configuration could explain the existence of trailing tidal stream. Furthermore, Sofue [48] considered the continuous ram pressure stripping in simulation of the Magellanic system, ignoring the presence of the SMC. Recently, the LMC–MW interaction without including the action of SMC has been studied, and the Stream’s properties have been successfully reproduced [65]. The assumption of ignoring the SMC is also motivated by the fact that the SMC’s impact on the orbital history of the LMC is minimal, because of $M_{LMC} \gg M_{SMC}$ [69]. Thus, the global dynamics of the LMC alone is sufficient for discrimination of gravity model. Since the aim of this study is examining the overall properties of the MS in the context of MOG and TeVeS, we use the single cloud model and ignore the presence of SMC.

In the modified gravity models, since we have ignored the Galactic halo, there is no significant dynamical friction on the MS, and the main factor in the stripping of the hydrogen from the MCs is the tidal force exerted by the Galactic disk.

Another simplifying assumption is the elongation of the MS. Although the formation of the MS is still a subject of debate, both the ram pressure and the tidal stripping models predict that the orbits of the Clouds should trace the MS at least for less than a Gyr in the past. In other words, the MS, as seen on the sky, is following the MCs and it is reasonable to assume that the MS is a narrow and long column of gas which is moving along the same orbit as the MCs [44, 45, 65, 69]. This assumption is motivated by the work by Johnston et al. [70], who suggested that the tidal stream acts as ”fossil record” of the recent orbital history of their progenitors and could thereby provide a probe of the galactic potential. In this way, the mean velocity of gas in the MS will be the orbital velocity of the MCs. In order to explain this assumption one can consider the dynamics of nearby satellites around the MW under the external tidal field [71, 72, 73, 74, 75]. There is a connection among the tidal tails and satellites’s orbits. After the formation and evolution of tidal tails around the satellite, the tails are aligned with the orbital path only when the satellite is near the perigalaction of the orbits [73, 74]. The degree of elongation of the tails along the satellite orbital path strongly depends on the ellipticity of orbit. In the circular orbit case, the tails are clear tracer of the cluster path, but for most eccentric orbits, the tails are strictly elongated along the orbital path only when the satellite is near the perigalaction, whereas at the apogalaction they tend to deviate from the satellite path [75]. Differently stated, in the case of eccentric orbits, the angle between tail and orbit decreases, when approaching the pericenter and reaches a minimum at the pericenter, and then increases moving away from it. Since the MCs are at the perigalaction, we assume that the stream is approximately elongated along the orbital path, and thus the mean velocity of gas would be the orbital velocity of the MCs. It must be noted that if the gas in the galactic halo itself moves,

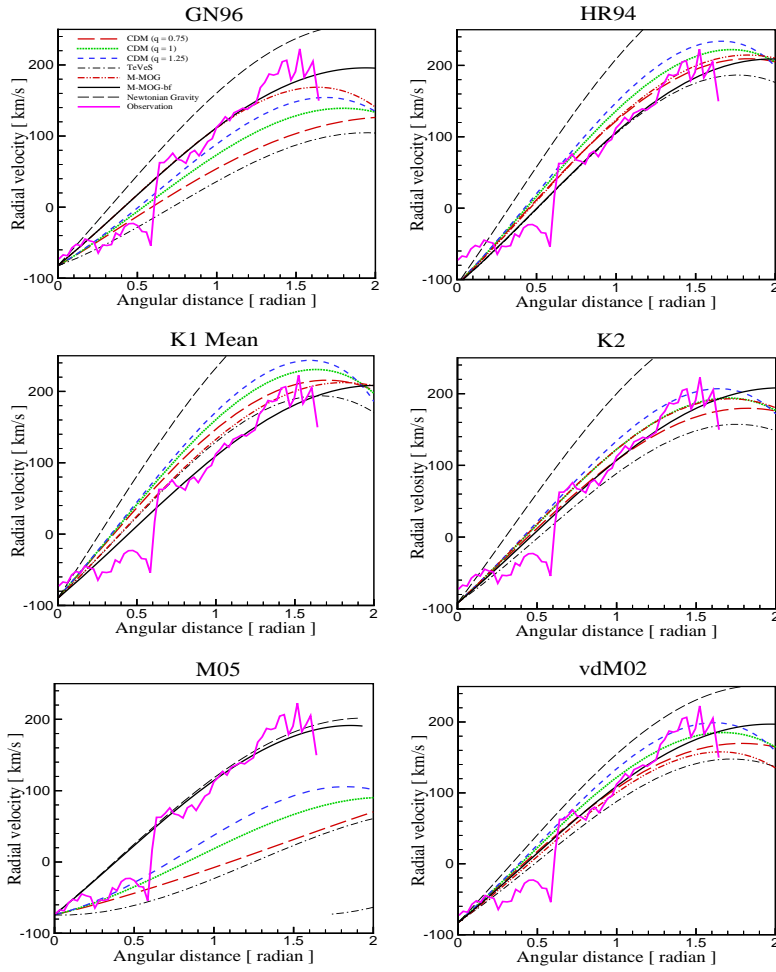


Fig. 1 The radial velocity versus the angular distance along the MS plotted for different galactic models and compared with the observational data. The results of the Newtonian gravity model without dark matter, the CDM halo for different values of q , and the best fit TeVeS model are indicated. The Moffat's modified gravity predictions in terms of the standard values of M_0 and r_0 (M-MOG) and with the best fit values (M-MOG-bf) are also presented. Each figure corresponds to one of the initial conditions listed in Table 1.

this effect can put the MS into almost any direction, making it impossible to use its dynamics to test CDM versus different gravity theories.

In the next section, we will use tidal scenario for the dynamics of MS obtaining the trajectories of the MCs in various gravitational models and comparing the radial velocity profile of MS with the observed data.

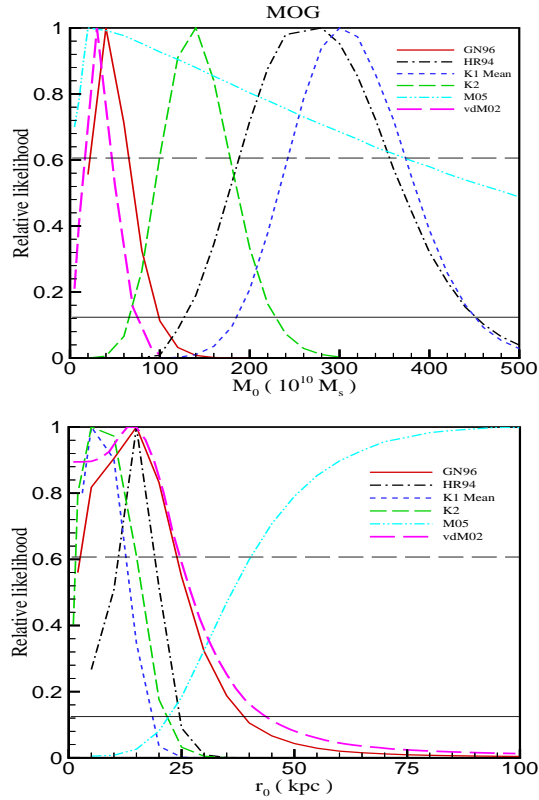


Fig. 2 Marginalized likelihood functions of the free parameters of MOG theory (r_0, M_0) for various initial conditions. The location of picks correspond to the best fit value of parameters. The intersection of the curves with the horizontal solid and dashed line give the bound at 1σ and 2σ confidence levels, respectively.

5 Results and discussion

The results of maximum likelihood analysis of the radial velocity profile of the MS for various gravity models, are presented in this section. One of the challenging points in calculating the orbital motion of the MCs is the initial conditions. The trajectory of the MCs is highly sensitive to the initial conditions, and slight variation may lead to completely different scenarios [34]. Furthermore, the parameter space of the Magellanic system evolution is very large [41, 42, 43, 44, 45]. Due to the implied numerical burden, doing the fully self-consistent simulation for each set of initial conditions and different combinations of parameters is impossible. Recently, an extended analysis of the parameter space for the interaction of the Magellanic system with the MW has been done [66]. They have used the genetic search algorithm and an approximate restricted N-body simulation method. Also in another orbital analysis, different sets of initial conditions have been used to determine the dynamics of the LMC [69].

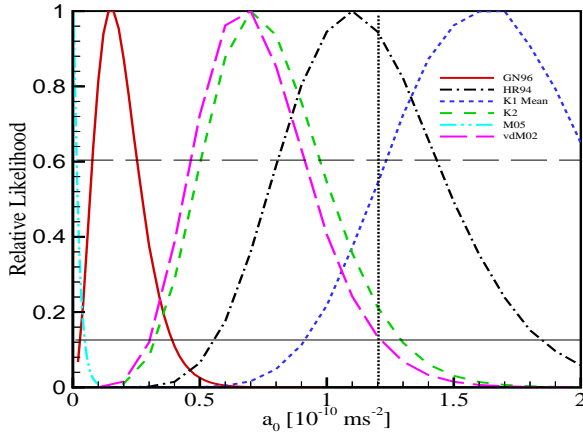


Fig. 3 Marginalized likelihood functions of the critical acceleration in TeVeS, for various set of initial conditions. The location of the picks correspond to the best fit values of parameters. The intersection of the curves with the horizontal dashed and solid line give the bounds at 1σ and 2σ confidence levels, respectively. The currently accepted value for $a_0 = 1.2$ on galactic scales are indicated by vertical dotted line. The predicted value of a_0 in the case of HR94 is in good agreement with the conventional value a_0 . Except GN96 and M05, the other initial condition predicts the acceptable value for a_0 at 2σ confidence levels.

We numerically integrate the equations of motion in 3D using the forth-order Runge-Kutta technique with a timestep of 0.5 Myr and total time of 5 Gyr. In MOG and TeVeS models, the radial velocity profile of the MS is extracted numerically for various initial conditions of the MCs listed in Table 1. In the next step we use χ^2 fitting to constrain the parameters of the model. Figure 1 compares the observed data with the theoretical predictions for various initial conditions. The data points represent the angular variation of observed radial velocity with respect to an observer located at the center of Galaxy [40]. The zero angular distance corresponds to the position of MCs center of mass. The models reproduce radial velocity of the stream as an almost linear function of angular distance with the high velocity tip reaching 200 km s^{-1} .

To test the consistency of MOG and TeVeS with observations, we compare their theoretical predictions to the data directly obtained from observations and find the best-fitting parameters. Since the agreement with the data cannot be perfect, we give confidence intervals for the free parameters of the model using likelihood analysis. We compute the quality of the fitting through the least-squares fitting quantity χ^2 defined by

$$\chi^2\{p_\alpha\} = \frac{1}{N} \sum_{i=1}^N \frac{(V_{theory}^i\{p_\alpha\} - V_{obs}^i)^2}{\sigma_i^2}. \quad (12)$$

where σ_i is the observational uncertainty in the radial velocity, N is the number of degrees of freedom ³ and p_α is the model parameters. In the case of MOG, $p_\alpha =$

³ $N = n - n_{p_\alpha}$, where n is the number of observational data points and n_{p_α} is the number of free parameters.

1	work	GN96	HR94	K2	K1 - Mean	M05	vdM02
2	χ^2_{NG}	16.4	63.9	50.3	90.7	2.5	13.3
3	χ^2_{MOG}	2.06	1.34	1.61	1.71	2.41	1.97
4	$r_0[kpc]$	15^{+8}_{-12}	15^{+5}_{-5}	5^{+12}_{-4}	5^{+10}_{-5}	$110^{+..}_{-60}$	13^{+11}_{-13}
5	$M_0[10^{10}M_\odot]$	40^{+25}_{-20}	280^{+80}_{-100}	140^{+40}_{-40}	300^{+80}_{-60}	20^{+360}_{-20}	30^{+20}_{-15}
6	$\chi^2_{TeV eS}$	2.2	1.35	1.8	2.12	2.38	2.39
7	$a_0[10^{-10}ms^{-2}]$	$0.15^{+0.08}_{-0.05}$	$1.13^{+0.32}_{-0.33}$	$0.7^{+0.25}_{-0.20}$	$1.7^{+0.30}_{-0.46}$	$0.01^{+0.01}_{-0.0}$	$0.72^{+0.20}_{-0.25}$
8	$\chi^2(q = 0.75)$	22.9	2.39	2.2	8.11	87	38
9	$\chi^2(q = 1)$	11.2	5.58	2.36	14.2	52	9.8
10	$\chi^2(q = 1.25)$	4.9	10.1	4.45	20.7	32	4.24
11	\bar{q}	1.7	0.4	0.7	0.2	2.7	1.43
12	$\chi^2_{CDM\bar{q}}$	1.61	1.67	2.0	3.1	2.83	1.9

Table 2 The best fit parameters of gravitational model and corresponding minimum values of χ^2 for different initial conditions (IC). The second row shows the χ^2 of the Newtonian gravity. The χ^2 and corresponding best fit parameters in MOG represented in rows of 3-5 as well as TeVeS in rows of 6 and 7. The error bars are obtained by marginalized likelihood analysis (Figures 2 and 3). The results of logarithmic CDM halo model for different values of q are shown in rows of 8-10. The last two rows indicate the best fit value of q and χ^2 for the logarithmic halo.

$\{r_0, M_0\}$ and in the case of TeVeS, $p_\alpha = a_0$. Using Eq. (12) we find the best fitted values of the model parameters that minimize $\chi^2\{p_\alpha\}$.

To constrain the parameters of the model, we carry out statistical analysis using the marginalized likelihood function defined by

$$\zeta\{p_\alpha\} = \xi e^{-\chi^2\{p_\alpha\}/2}, \quad (13)$$

where ξ is a normalization factor. The marginalized likelihood function of the model parameters are plotted in Figures 2 and 3. According to Eq. (13), the maximum values of ζ correspond to the minimum values of χ^2 . Therefore, the location of the peaks correspond to the best fitted values of the parameters. The main benefit of using the ζ function is in finding the 1σ (68.3 %) and 2σ (95.4 %) confidence intervals of best-fitting values of the parameters. The best-fitting values for the parameters of the model at 1σ and 2σ confidence intervals for various initial conditions are shown in Figures 2 and 3. The best-fitting values for the parameters of the model at the 1σ confidence interval with the corresponding χ^2 are presented in Table 2.

The second row of Table 2 shows the χ^2 of Newtonian gravity considering the only baryonic matter for Galaxy. As we expect, the values of χ^2 are very large which means that we need the dark matter or modification of gravity. The most interesting result is that the initial condition M05 is almost compatible with the observation due to the low value of χ^2 , which predicts very small amount of dark matter for the galaxy.

In MOG model we apply the likelihood analysis to find the best values of the mass scale M_0 and range parameter r_0 . The minimum values of χ^2 and corresponding best fit parameters are represented in the rows of 3-5. The error bars obtained by marginalized likelihood analysis (Fig. 2). According to the values of M_0 and r_0 in section 3 which were obtained from fits to satellite galaxies and rotation curves of galaxies, the reasonable ranges for Magellanic system would be in the range of $[90 - 5000] \times 10^{10}M_\odot$ for M_0 and $[14 - 111]$ kpc for r_0 . However, the obtained best fit values of r_0 are almost in the acceptable range for all sets of initial conditions, but the M_0 values are out of range in the case of GN96 and vdM02 (see Table 2). Furthermore, the values of r_0 and

M_0 in K1-Mean and M05 do not follow Eq. (5) which postulated in MOG theory even considering the error bars. The case of HR94 is in excellent agreement with observation, because of the reasonable best fit parameters and the smaller value of χ^2 . Therefore, we can conclude that, the MOG theory could be compatible with the observational feature of MS by choosing the appropriate values for free parameters and for special sets of initial conditions of the MCs.

In the TeVeS model, with the standard value of the acceleration scale, $a_0 = 1.2 \times 10^{-10} \text{ ms}^{-2}$, except HR94 which reached a low χ^2 value, the other initial conditions are not compatible with observations. However, the value of a_0 has been fixed from rotation curve analysis by Begemann et al. (1991)[12], it is worth to obtain the value of a_0 from some other independent method. Moreover, among the MOND community there is no common idea about the value of a_0 at different scales. At different scales like clusters of galaxies or small dwarf galaxies, it seems the standard value of a_0 does not give acceptable results. At large scales, a lower value of a_0 , and at subgalactic scales a larger value of a_0 work better [79, 80, 81, 82]). In this paper, since we are studying the dynamics of MCs, i.e. local group scale, it is probable to find another best-fit value for a_0 . For this reason, in order to see the effect of different choice of a_0 , we allow a_0 to changes and find a best-fit a_0 for each initial condition which gives the better fit with observation.

Figure 3 depicts the best fit values of a_0 for different initial conditions. Except models GN96 and M05 which prefer a small value of a_0 , for the other initial conditions (Table 2), the best fit value of a_0 are almost in agreement with standard value. Thus, in the TeVeS model, GN96 and M05 are ruled out due to their strange perdition for a_0 .

In order to compare the results with the CDM models, we apply the same analysis for the logarithmic halo model. We adopted different values for halo flattening parameter to deal with prolate, oblate and spherical halos. According to Table 2, the minimum values of χ^2 belong to HR94 and K2. They prefer the oblate and spherical halo models ($q = 0.75 - 1$). According to the last row, HR94, K2, and K1-Mean prefer oblate halos whereas, GN96, M05 and vdM02 prefer the prolate ones. In addition, the minimum values of χ^2 , in the CDM model for GN96 and HR94, are comparable with MOG and TeVeS, which means that the alternative gravity models can successfully explained the observational velocity profile as well as the CDM halo models.

According to the minimum values of χ^2 for different gravity models in Table 2, for the majority of initial conditions, the MOG model fit the observations better. However, the difference is not enough to discriminate between different gravity models.

6 Conclusion

In our paper we test alternative gravity models by comparing of the radial velocity profile of the Magellanic Stream (MS). We numerically integrated the orbits and dynamics of the Magellanic Clouds (MCs) within different gravitational models. The MS is produced by the interaction of the MCs with the Galaxy, and is considered to be a tracer of the MCs. The drag force plays no significant role in the orbital motion of the Clouds. In the absence of the dark halo of the Milky Way, since the Clouds move outside the visible mass distribution, there is no dynamical friction in the equations of motion. We used the single cloud model and ignore the presence of the SMC. The gravitational tidal effect of Galaxy is assumed as the origin of the MS and it follow the

same orbit with the same dynamics as the LMC. The radial velocity of this structure is compared with the observation, allowing us to put constraints on the free parameters of models.

A preliminary inspection of the fits to the Magellanic Stream showed that for some individual initial conditions, the MOG theory, choosing the appropriate values of free parameters, r_0 and M_0 , can be consistent with the observational velocity feature of MS, as well as TeVeS, and CDM hypothesis. However, due to small difference in minimum values of χ^2 , the discrimination between different gravity models is impractical. The fits to the Magellanic Stream based on the parameters M_0 and r_0 of the older study of STVG, reveal that the new parameter-free version of STVG [26] appears to agree well with the results presented in this paper.

We should point out that while the dynamics of the MS is in a good agreement with observations, a problem with tidal scenario could be the lack of corresponding stellar tidal debris in the MS. In TeVeS and MOG, since the tidal radius is larger than of the Newtonian case, we expect a Galactic structure with a gas distribution that is more extended than the stellar component form of the MS. N-body simulations of tidal stripping of the MS from the MCs in MOG without dark matter will give a better view of this model and enable us to compare the density distribution of the gas in the MS with observations. As an additional result it seems that the initial condition HR94, is in a good agreement with observation in all gravitational models.

Acknowledgements We thank Alireza Moradi for useful comments on the English of paper.

References

1. Bosma, A. 1981, AJ, 86, 18251846.
2. Rubin, V. C., and Burstein, D., 1985, ApJ, 297, 423435.
3. Spergel D. N. *et al.*, 2007, ApJS, 170, 377.
4. Moore B. *et al.*, 1999, ApJ, 524, L19.
5. Klypin A. *et al.*, 1999, ApJ, 522, 82.
6. Grebel E.K., Gallagher J.S., 2004, ApJ, 610, 89
7. Ishiyama, T., Fukushige, T., Makino, J., PASJ, 2008, 60, 4, L13–L18
8. Ishiyama, T., Fukushige, T., Makino, J., ApJ, 2009, 696, 2115
9. Simon, J. D., Geha, M., ApJ, 2007, 670, 313
10. Milgrom M., 1983, ApJ, 270, 365
11. Bekenstein J.D., Milgrom M., 1984, ApJ, 286, 7
12. Begeman K.G., *et al.*, 1991, MNRAS, 249, 523
13. Sanders R. H., McGaugh S., 2002, ARAA, 40, 263.
14. Bekenstein J., 2004, PRD, 70, 083509
15. Clowe, D., *et al.*, 2006 ApJ, 648, L109.
16. Angus, G.W., Famaey, B. and Zhao, H.S., 2006 MNRAS, 371, 138
17. Moffat J. W., Phys. Letts. B 355, 447 (1995)
18. Moffat, J. W. 2005 JCAP 2005, 003
19. Moffat, J. W. 2006 JCAP, 2006, 004
20. Moffat, J. W., & Sokolov, I. Y., 1996, Phys.Lett.B, 378, 59, arXiv:astro-ph/9509143.
21. Moffat, J. W., & Toth, V. T., arXiv:0710.0364.
22. Moffat, J. W., & Toth, V. T., 2009, MNRAS, 395, L25–L28, arXiv:0710.3415.
23. Moffat, J. W., & Toth, V. T., arXiv:0805.4774, accepted in MNRAS.
24. Moffat, J. W., & Toth, V. T., 2009, ApJ, 680:1158, arXiv:0708.1935.
25. Moffat, J. W., & Toth, V. T., arXiv:0708.1264.
26. Moffat, J. W., & Toth, V. T., 2009, Class. Quantum Grav, 26, 085002, arXiv:0712.1796.
27. Moffat, J. W. 2006, (gr-qc/0608074).
28. Brownstein, J. R. and Moffat, J. W., 2006 ApJ, 636, 721.
29. Brownstein, J. R. and Moffat, J. W., 2006 MNRAS, 367, 527.

30. Brownstein, J. R. and Moffat, J. W., (astro-ph/0702146).
31. Haghi, H., Rahvar, S., Hasani, Z. A., 2006, ApJ, 652, 354
32. Haghi, H., Hasani, Z. A., Rahvar, S., 2009, New Astronomy, 14, 692699.
33. Haghi, H., Baumgardt, H., Kroupa, P., Grebel, E. K., Hilker, M., & Jordi, K., 2009, MNRAS, 395, 1549.
34. Iorio, L., 2010, MNRAS, 401, 2012, arXiv:0904.0219v1 [gr-qc]
35. Iorio, L., 2009, Astron. Nachr., 330, 857-862
36. Iorio, L., 2008, Scholarly Research Exchange, vol. 2008, Article ID 238385
37. Wannier P., Wrixon G. T. 1972, ApJ, 173, L119.
38. Mathewson D. S., Cleary M. N., Murray J. D. 1974, ApJ, 190, 291.
39. Mathewson D. S., et al., 1987, Proc. Astr. Soc. Aust. 7, 19.
40. Brüns, C., et al. 2005, A&A, 432, 45.
41. Fujimoto, M., Sofue Y., 1976, A&A, 47, 263.
42. Murai T., Fujimoto M., 1980, PASJ, 32, 581.
43. Lin D. N. C., Lynden-Bell D. 1982, MNRAS 198, 707.
44. Gardiner, L. T., Sawa, T., and Fujimoto, M. 1994, MNRAS, 266, 567
45. Gardiner, L. T., Noguchi, M. 1996, MNRAS, 278, 191.
46. Moore B., Davis, M. 1994, MNRAS 270, 209.
47. Heller P., Rohlfs K., 1994, A&A, 291, 743.
48. Sofue, Y. 1994, PASJ, 46, 431.
49. Evans N. W., 1994, MNRAS, 267, 333.
50. Kuzmin G. G., 1956, AZh, 33, 27
51. Brada R., Milgrom M., 1995, MNRAS, 276, 453
52. Johnston K., Majewski S., Siegel M., Reid I., Kunkel W., 1999, AJ, 118, 1719
53. Law D., Johnston K., Majewski S., 2005, ApJ, 619, 807
54. Read J., Moore B., 2005, MNRAS, 361, 971
55. Kochanek, C. S., 1996, ApJ, 457, 228
56. Helmi, A. 2004, MNRAS, 351, 643
57. Binney S., Tremaine S. 1987, Galactic Dynamics, Princeton Univ. Press, Princeton, NJ.
58. Famaey B., Bruneton J., & Zhao H.S., 2007, MNRAS, MNRAS, 377L, 79
59. Wu, X., et al., 2007, ApJ, 665, L101, (arXiv:0706.3703v2)
60. Gentile G., Famaey B., Combes F., Kroupa P., Zhao H.S., & Tiret O., 2007, A&A, 472, L25.
61. Wu, X., et al., 2008, accepted for publication in MNRAS, (arXiv:0803.0977v1).
62. Weinberg, M, D. 2000, ApJ, 532, 992.
63. Connors, T.W., Kawata, D. & Gibson, B.k. 2006, MNRAS, 371, 108
64. Meurer, G. R., Bicknell, G. V., Gingold, R. A. 1985, PASA, 6, 2, 195
65. Mastropietro C., et al., 2005, MNRAS 363, 521.
66. Ruzicka, A., Palous, J., Theis, C. 2007, A&A, 461, 155.
67. Lin D. N. C., Lynden-Bell D., 1977, MNRAS, 181, 59-81.
68. Liu, Y. 1992, A&A 257, 505.
69. Besla, G., et al., 2007 (astro-ph/0703196).
70. Johnston K. V., et al, 1999, ApJ, 512, L109.
71. Martinez-Delgado D., et al., 2004, (astro-ph/0409118)
72. Murali C., Dubinski J., 1999, AJ, 118, 911
73. Dolcetta R. C., Di Matteo P., Miocchi P., 2005, AJ. 129, 1906
74. Odenkirchen, M., et al. 2003, AJ, 126, 2385.
75. Montuori, M., et al. 2007, ApJ, 659, 1212.
76. Kallivayalil, N., van der Marel, R. P. and Alcock, C. 2006b, ApJ, 652, 1213, [K2]
77. Kallivayalil, N., et al., 2006a, ApJ, 638, 772, [K1]
78. van der Marel, R. P., Alves, D. R., Hardy, E., & Suntzeff, N. B., 2002, AJ, 124, 2639, [vdM02]
79. Lokas, E. L., 2001, MNRAS, 327, 21
80. Nusser, A., 2002, MNRAS, 331, 909
81. Sanders, R.H., 2005, MNRAS, 363, 459
82. Bekenstein, J. D., Sagi, E., 2008, PhRvD, 77, 10, 103512